Environmental DNA reveals differential geologic isolation effects on plant and fungal Communities in the Hengduan Mountains

Yaquan Chang[1,2,3], Yifan Wang[4], Xianjun Fang[3], Ao Luo[5], Wenjun Zhong[4], Xiaowei Zhang[4], Zhiheng Wang[5], Camille Albouy[1,2], Niklaus E. Zimmermann[2], Sean D. Willett[3], Loïc Pellissier[1,2]

1. Ecosystems and Landscape Evolution, Department of Environmental Systems Science, ETH Zürich

2. Land Change Science Research Unit, Swiss Federal Institute for Forest, Snow and Landscape Research (WSL)

3. Earth Surface Dynamics, Department of Earth and Planetary Sciences, ETH Zürich

4. State Key Laboratory of Pollution Control & Resource Reuse, School of the Environment, Nanjing University, Nanjing 210023, P. R. China

5. Institute of Ecology and Key Laboratory for Earth Surface Processes of the Ministry of Education, College of Urban and Environmental Sciences, Peking University, Beijing, 100871 China

Corresponding author: Yaquan Chang; yaquanchang0623@gmail.com

Abstract

Species range limits are typically constrained by their tolerance to abiotic factors such as climate, as well as by dispersal limitations due to geographic barriers like mountain ridges and river valleys. Montane regions, which are hyperdiverse in many different clades, characterised by high turnover, and complex topography, provide ideal systems for investigating the drivers of range limits. In this study, we collected 30 environmental DNA (eDNA) samples from the tributaries of the Salween, Mekong, and Yangtze rivers in west China and employed ITS2 primers to analyse the species phylogenetic beta diversity of plant and fungal communities. We then applied a null model approach to disentangle the dispersal limitation process from the climate filtering process. Habitat preference analyses indicate that our eDNA samples predominantly capture mid-to-low elevation species. The spatial pattern of the PCoA plot from phylogenetic beta diversity revealed congruent distribution patterns between plant and fungal groups, with assemblage segregation across different river valleys and along latitudes. The plant communities were structured along the Salween-Mekong divide once climatic and distance effects were accounted for. Our results highlight the efficiency of using river eDNA to detect the terrestrial plant and fungi communities and emphasize the dispersal barrier is taxa and location dependent.

Keywords:

Environmental DNA, plant, fungi, geographic barriers, climate filtering

Introduction

Mountain regions harbour disproportionate terrestrial biodiversity globally despite occupying only 25% of the land area [1]. This high biodiversity level is caused by the aggregation of many small-range species [2] with species composition varying substantially over short geographic distances [3], or along elevational gradients [4,5] or across river valleys [6]. Thus, examining species assemblage replacement (hereafter: beta diversity) across geographic distance is essential for understanding the biodiversity distribution of the montane systems. Environmental filtering and dispersal limitation are two primary mechanisms in driving community composition. Environmental filtering determines species range limits based on abiotic control, constraining species range limits according to environmental conditions such as temperature [7,8] and precipitation [9,10]. This hypothesis suggests that current climatic variations could influence species range limits due to species-habitat associations [11]. In addition, geographic barriers can impede species dispersal even within similar abiotic conditions, eventually leading to long-term isolation and subsequent allopatric speciation [12]. For example, the interfluvial drainage divide generated from escarpment retreat created dispersal barriers for vascular plants in Madagascar [13]. Montane regions with high levels of complex topography have restricted species dispersal and thus host a high number of small-ranged species [2,12]. However, these hypotheses are not mutually exclusive and have strong interactions. For example, mountain ranges also act as barriers to atmospheric moisture, creating rain shadows and filtering drought tolerant species on one side of mountain ranges. The complex topography further compresses diverse climates within short geographic distances along elevational gradients, further filtering species that favour different environmental conditions, promoting high spatial species turnover in montane regions [14]. Therefore, disentangling the role of dispersal barriers from climate filtering is essential to understand how mountain ranges play a role in geographic isolation.

Mountain regions have been identified as phylogeographic hotspots, where phylogeographical patterns often correspond with geographic features such as mountain ridges [15] and river valleys [16]. These geographic features can block gene flow among populations, eventually leading to allopatric speciation across clades. For example, high mountains, lacking low-elevation passes have been identified as dispersal barriers for birds [17], mammals [18], amphibians [15], and plants [19]. The effectiveness of these barriers, however, may also depend on species' habitat preferences and dispersal abilities [12]. Moreover, mountain ridges have been shown to impede the population connectivity of mid-to-low elevation yews [20], while deeply incised river valleys can act as dispersal barriers for alpine clades, isolating mountain peaks as sky islands [21]. Moreover, life history traits related to dispersal, such as avian wing size [12], plant seed size [22], or belonging to functional groups [23], also influence how species interact with these barriers. For example, mountainous barriers pose less of an obstacle to ferns compared to other plants due to their easily dispersed spores [24]. Therefore, considering habitat preferences and functional groups can enhance our understanding of the role and effectiveness of geographic features as dispersal barriers.

The environmental DNA (eDNA) metabarcoding approach enables rapid and efficient biodiversity monitoring, particularly for the quick characterisation of riverine species, as it can simultaneously detect multiple taxa through the use of primers [25]. Riverine eDNA is extensively employed to identify freshwater fish [26,27] and vertebrates [28]. However, the evaluation of terrestrial plant and fungi communities through riverine eDNA has been much less studied [29], despite rivers transporting plant fragments such as pollen, leaves, or flowers [30]. Detecting plant diversity in riverine environments is challenging due to the trade-off between the prevalence and length of eDNA fragments [31]. The high occurrence of small DNA fragments in water samples often leads to an elevated read abundance of short amplicons. The plant eDNA requires larger metabarcoding markers (over 500 bp) to distinguish closely related species, which is present in lower quantities [31]. This makes it difficult to detect a sufficient number of plant and fungi species in rivers. The nuclear ribosomal DNA (nrDNA) internal transcribed spacer-2 (ITS2) region has been identified as an effective genetic marker for flowering vascular plants due to its high mutation rate and conserved small size (220 bp; Espinosa Prieto et al., 2024). This makes ITS2 a valuable target for detecting terrestrial plants and fungi in eDNA studies. While ITS2 has been widely used to detect plant and fungi communities in the soil [32], and airborne [33], it has rarely been assessed in riverine eDNA [30]. Therefore, it is essential to expand the assessment of the ITS2 primer for plants and fungi using riverine eDNA, as the extent to which river eDNA can accurately capture terrestrial plant and fungal diversity remains largely unexplored.

Situated at the tectonic boundary between the Indian and Eurasian plates, the Hengduan Mountains (HDM) region is recognised as a major biodiversity hotspot outside the tropics. The Three Rivers Region (TRR) stands out in the HDM due to its complex topography and exceptional biodiversity [34]. The Salween, Mekong, and Yangtze rivers, originating from Tibet, run north to south in roughly parallel paths, carving deep gorges up to 3000 metres deep and coming within tens of kilometres of each other at their closest points [35]. The TRR is characterised by numerous north-south oriented mountain ranges with extreme relief, dissected by river valleys, leading to a fragmented landscape with repeated ridge-valley patterns [36]. This creates an ideal natural laboratory for studying how geographic features influence phylogeographical discontinuities. For example, the TRR has been shown to hamper gene flow among populations and amplify speciation in plants [20], and amphibians [37]. While the north-south oriented river valleys in the TRR provide potential corridors for dispersal across latitudes, rapid species turnover near the TRR bottleneck around 28°N suggests that climate gradients, particularly winter temperatures, significantly influence species distributions [38]. A comprehensive, multi-taxa investigation based on eDNA sampling can help determine to what extent these repeated geographic features play the dispersal barriers in the TRR region.

In this study, we evaluate the effectiveness of mountain ridges and river valleys as dispersal barriers by analysing the phylogenetic composition of plant and fungi species across 30 drainage basins in the tributaries of the Salween, Mekong, and Yangtze Rivers using eDNA. We constructed plant and fungi communities based on water samples from each tributary. We first assessed the sampling efficiency by comparing the elevation range of sampled plants and

that of the drainage basins. Next, we investigated the spatial pattern of species phylogenetic beta diversity in the TRR including construction of a generalized dissimilarity model to quantify the impact of climate. Finally, we examined whether mountain ridges play the role as dispersal barriers after controlling for the effect of the climate filtering process. Specifically, we addressed the following questions:

1) Can current sampling methods cover the whole drainage basin? Which elevation bands are sampled by the riverine eDNA samples from tributary outlets?
2) What are the spatial distributions of plant and fungi phylogenetic diversity? Do they show congruent distribution patterns?
3) Do mountain ridges act as dispersal barriers for both plant and fungi communities after controlling the climate filtering process?

Results

Taxonomic assignment

After the taxonomic assignment and cleaning step, the total number of reads in the ITS2 was 1,653,080 (average reads/filter =27,099.67 ± 28,088.96) across the 61 pooled eDNA samples. Plant species were detected in 29/30 sites, with 33 ASVs assigned to the family level, 139 ASVs assigned genus level and 105 ASVs to the species level. After assigning to the global genus level phylogenetic tree, 134 genera were retained to perform the analyses. In the Salween valley, Urticaceae was particularly diverse, the number of genera detected occupying 9% of the total detected genera (Figure S2). The Salween River also has high proportions of Araliaceae and Saxifragaceae (6.0% and 4.5% respectively), while the Mekong and Yangtze rivers do not. The Yangtze and Mekong rivers share the same top 4 families including Fabaceae, Asteraceae, Urticaceae, and Poaceae while the orders are slightly different. Fungal species were detected at 27 out of 30 sites, encompassing 46 orders and 88 families. Pathogenic and nonyeast unicellular fungi are the dominant functional groups among all rivers. The Salween River has a high abundance of yeast, while the Mekong and Yangtze rivers have a high abundance of opportunistic human pathogens (Table S3). The detailed site level checklist for plants and fungi could be found in Figure S2 and S3 respectively.

Sampled habitats for plant communities

The elevation gradient of sampled drainage basins ranged from 2123.9 ± 290.3 m to 4278.7 ± 565.0 m, with a mean elevation of 3201.3 ± 390.4 m and an elevation range of 2154.8 ± 444.1 m (Figure 2). The plant elevational preferences show the maximum (Figure 2), mean (Figure S5), and minimal (Figure S6) elevation density for all plant genera found in certain drainage basins. The mean elevation of the maximum elevation preference across all drainage basins is 2347.8 ± 304.8 m (Figure 2). Comparing the plant maximum elevation preference with the whole elevational gradient of the drainage basin, the plant elevation preference shifts towards a lower elevation of 853.5 ± 473.2 m (Figure 2). The overlap between species' maximum elevation range and basin elevation was 51.6% ± 19.1%. Additionally, the plant mean and minimal preferred elevation maps showed downward shifts of 1303.2 ± 449.1 m (Figure S5) and 1719 ± 466 m (Figure S6), respectively. The overlap of plant mean and minimal preferred elevations with the drainage basin elevations were 29.5% ± 15.5% (Figure S5) and 14.1% ± 9.2% (Figure S6), respectively.

Spatial pattern of species composition

The first two axes of the Principal Coordinates Analysis (PCoA) explained 45.5% and 58.5% of the variance for plants and fungi, respectively (Figure 1b, d). The spatial pattern of the first two PCoA axes delineated distinct east-west and north-south gradients of phylogenetic beta diversity (Figure 1). The Salween River showed a more distinct species composition compared to the Mekong and Yangtze rivers for both plant and fungi groups (Figure 1, S2, S3). In the plant community, the Salween River is dominated by some tropical genera such as Toxicodendron, Tetracentron, Ficus, Maclura, Pilea (Figure S2). In the fungi community, some tropical families and functional groups have been mainly found in the Salween River such as schizoporaceae, polyporaceae (Figure S3). The latitudinal gradient of the PCoA pattern indicated a significant turnover at ca. 28°N, with this transition occurring further north in the Salween and further south in the Yangtze (Figure 1).

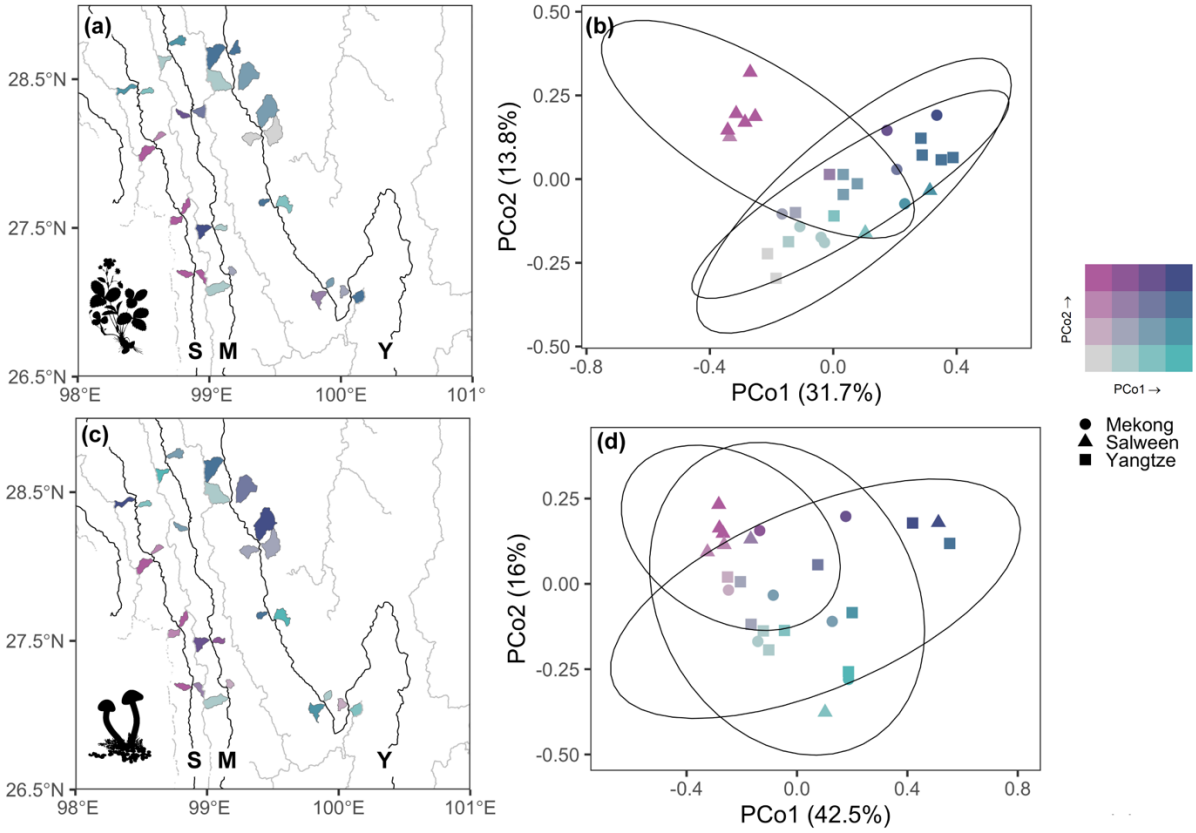

Figure 1. Species composition of vascular plants and fungi on biplot maps and pcoa ordinary plots based on Sorensen phylogenetic beta diversity. Figures (a) and (c) represent the spatial distribution of the first two PCoA axes in plants and fungi, respectively; colour gradients highlight the species composition difference between different drainage basins. Black lines represent the river valleys and grey lines represent mountain ridges. S represents the Salween River, M represents the Mekong River, and Y represents the Yangtze River. The second column represents the PCoA ordination of species composition in the Salween, Mekong and Yangtze Rivers. The colour of the points corresponds to the color in the drainage basins in the left panel. Circles represent the Mekong River, triangles the Salween River, and squares the Yangtze River. Data ellipses were computed for the ordination plot considering a multivariate t-distribution with a 0.95 level. The silhouette images were derived from phylopic (https://www.phylopic.org).

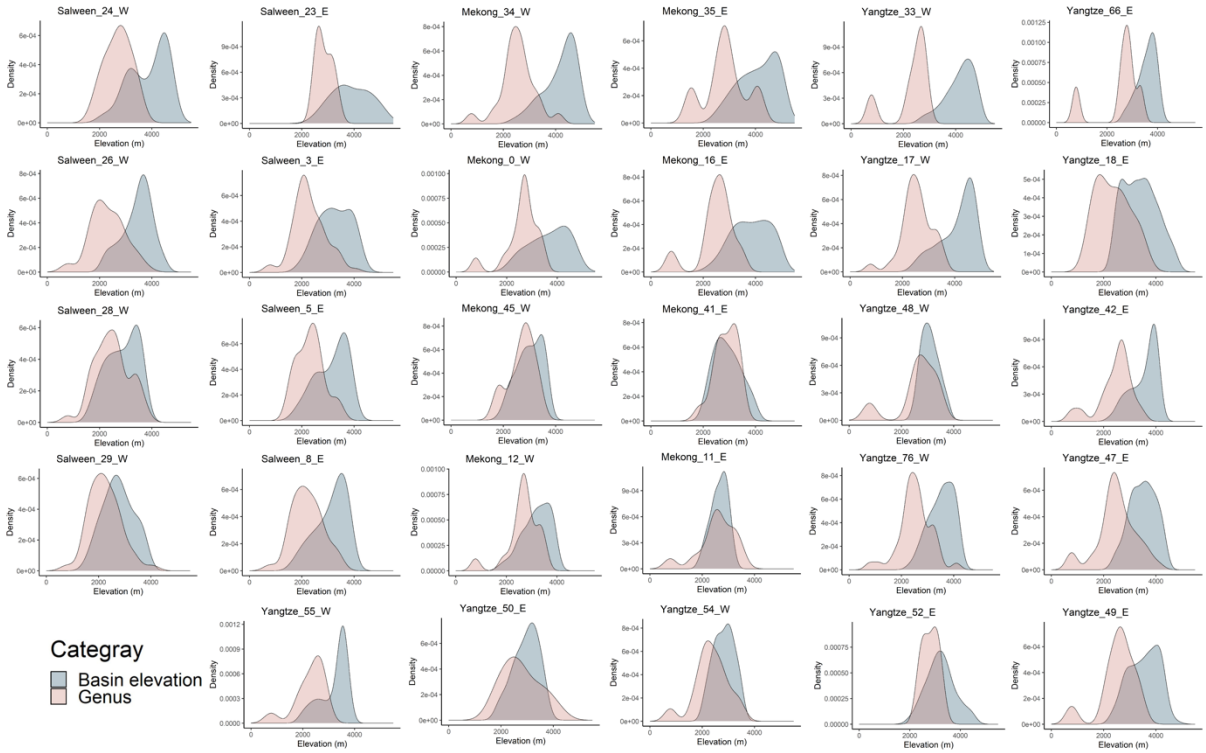

Figure 2. Elevation density plots with the sampled genus maximum elevation preference in each drainage basin (pink) and the full gradient of elevation of whole drainage basins (grey), in all sampling sites across Salween, Mekong and Yangtze Rivers.

Elevational profile and phylogenetic beta diversity of the Three-River Region

The geomorphic analysis reveals significant elevational changes from west to east in the TRR region that have a corresponding relationship in the phylogenetic beta diversity. The structure of the geography is dominated by the north-south flowing rivers and their intervening divides, which provide potential dispersal barriers. The relief of the Salween-Mekong divide is larger than the Mekong-Yangtze and the distance between the Salween and Mekong rivers is consistently smaller (Figure 3). Along the south and north swathes, both divides have an elevation increase from 3700 m to 5000 m. The phylobeta diversity along the east-west elevational profiles generally reveals significant high beta at the main divides than phylobeta in the river valleys across plant ($p < 0.01$) and fungal ($p = 0.058$) although the most north profile shows an opposite trend where phylobeta in the Salween River (0.600 and 0.812 for plant and fungi groups respectively) is higher than phylobeta in other river valleys and ridges.

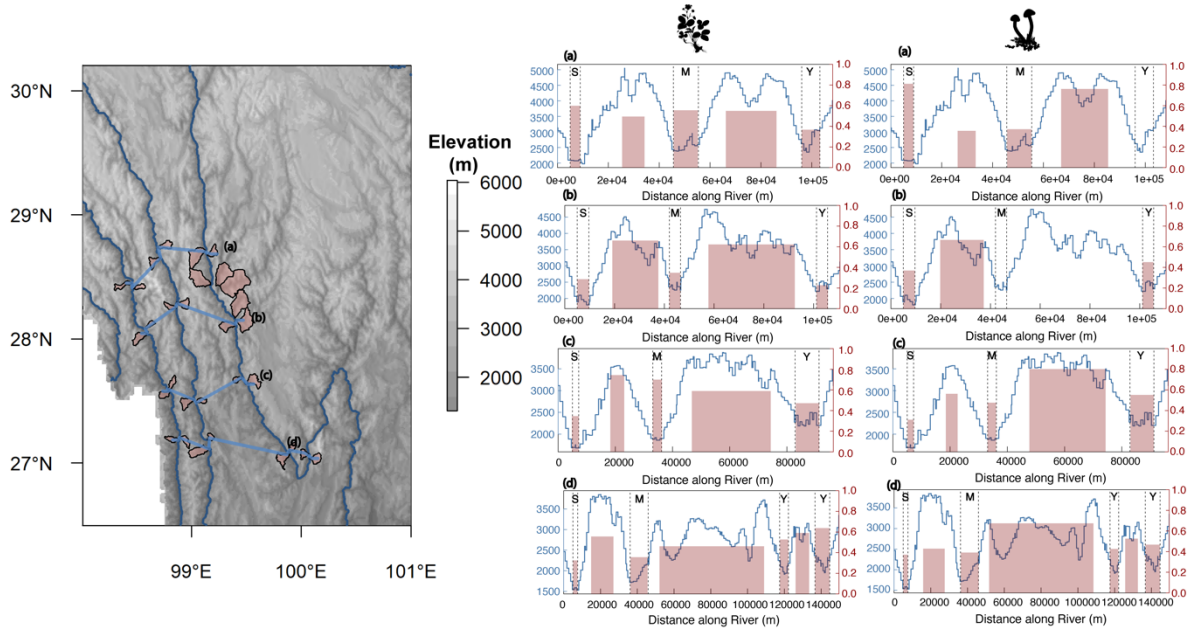

Figure. 3. The phylogenetic beta diversity along different swathes. Dark blue lines in the left map represent the main trunks. The blue transects represent four swathes across sampling sites in the right panels. The polygons in the map represent the corresponding drainage basins. In the right panels, pink bars represent the phylogenetic beta diversity between two adjacent basins, and blue lines represent the elevation profile along the swath. The silhouette images were derived from phylopic (https://www.phylopic.org).

Impact of climate isolation on phylogenetic beta

In the null model, the climate and geographic distance jointly explain the beta diversity with an explanation power that varied from 6.21% to 17.98% (Table S4). The GDM model has a consistent higher explanatory power in the plant community than the fungi community in both taxonomic and phylogenetic beta diversity (Table S4). PC2 is the most important predictor in these communities (Table S4), reflecting precipitation seasonality, annual range of air temperature, mean monthly precipitation amount of the coldest quarter, min daily min temperature of the coldest month, precipitation amount of the driest month (Figure S7). The PC1 is the second predictor, mainly reflecting monthly near surface relative humidity, site water balance, vapor pressure deficit, climate moisture index, and first day of the growing season (Figure S7).

The divide isolation impact after accounting for climate on beta diversity

The observed beta diversity crossing drainage divides is significantly higher than predicted beta diversity from climate difference. But this pattern varied across different groups and different divides (Figure 4). For the plant group, the Wilcoxon t-test shows a significant difference between the observed pattern of phylogenetic beta is significantly higher than the predicted beta diversity in the Salween-Mekong and Salween Yangtze divides ($p < 0.001$, Figure 4a) but not in the Mekong-Yangtze divide. In contrast, in the fungi community, none

of the divides revealed a significant difference between climate predictions and observed phylobeta (Figure 4b). The plant community has a consistent pattern when comparing taxonomic beta diversity, revealing the observed beta diversity is significantly higher than predicted beta diversity from pure climatic model in Salween-Mekong ($p < 0.001$, Figure S8a) and Salween-Yangtze ($p < 0.001$, Figure S8a) divides. In the fungal community, all divides show non-significant differences between observed taxonomic beta and predicted taxonomic beta except the Salween-Yangtze divide. The Salween-Yangtze divide shows a significantly higher observed taxonomic beta than predicted taxonomic beta diversity from climate effects ($p < 0.01$, Figure S8b).

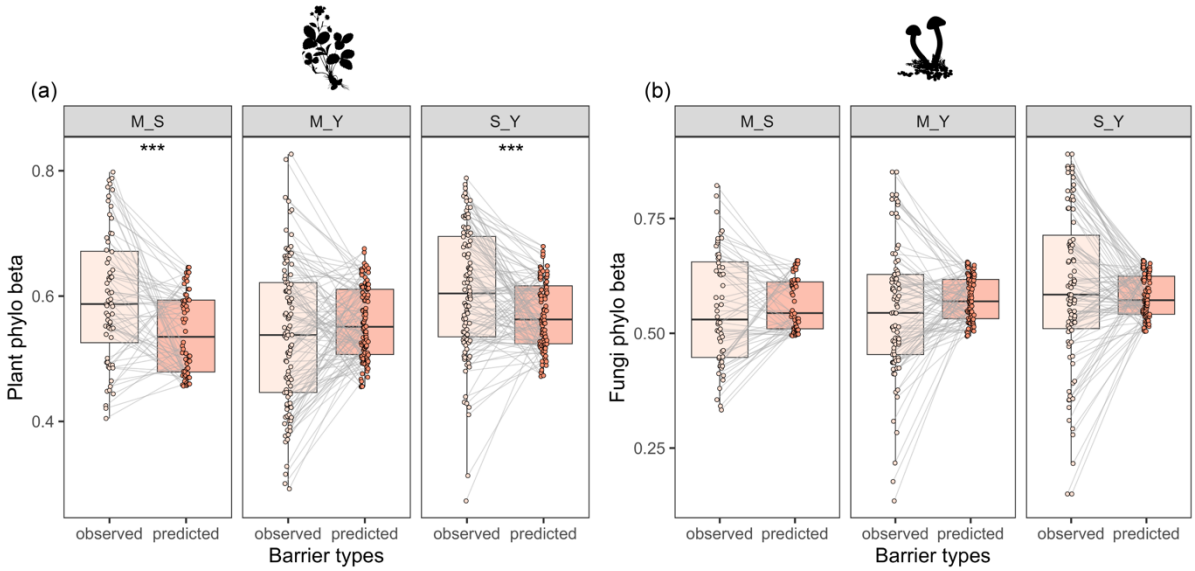

Figure 4. The pairwise comparison between climate and geographic distance predicted phylogenetic beta diversity versus observed phylogenetic beta diversity across different mountain ridges in both plant (a) and fungi (b) communities. Note that M_S represents the Salween-Mekong drainage divide; M_Y represents the Mekong-Yangtze divide; and S_Y represents the Salween-Mekong-Yangtze divide. Star signs represent the significance level from Wilcox comparison (i.e. p<0.001***; p<0.01**; p<0.05*). The silhouette images were derived from phylopic (https://www.phylopic.org).

Discussion

Temperate mountain regions are typically associated with high species turnover [3], largely due to climate filtering and dispersal limitation processes [39]. In the Hengduan region, we found the north-south oriented mountain ranges play a significant role in impeding species dispersal in east-west directions. The clear segregation of plant and fungal phylogenetic beta diversity observed in both PCoA analyses and elevational profiles underscore the association between high phylogenetic turnover and mountain ridges. This highlights the function of mountain ridges acting as dispersal barriers. The rapid incision of the rivers in the TRR region has raised north-south oriented parallel mountains ranges [35], encouraging species to migrate in the north-south direction while restricting east-west genetic exchange among populations and leading to distinct geographic assemblages from east to west. For example, the tropical clade of Urticaceae, originally from the tropical region, primarily migrated northwards through the

Salween River valley [40]. The role of mountain ridges as dispersal barriers is observed elsewhere. For instance, mountain range configurations have been linked to phylogenetic discontinuities in the Andes [6], and Rocky Mountains [17] across various taxa, including birds [17], plants [19] and mammals [41]. Spatial congruence analyses revealed two main mechanisms by which mountain ridges drive species turnover. First, the climate filtering process plays a key role in driving species turnover in mountain systems [42]. The strong elevation gradient is associated with a temperature gradient, and mountain ridges act as barriers to moisture, creating precipitation gradients and rain shadows, resulting in dramatic precipitation gradients on both sides of a mountain ridge [43]. These climatic gradients filter species based on their temperature and drought tolerance [20,44]. This process is particularly prominent in the Hengduan Mountains, where north-south ridges shape the south Asia monsoon system by blocking eastward cyclonic flow, producing a pronounced west-to-east precipitation gradient [45]. Secondly, mountain ridges can act as direct geographic barriers, physically obstructing species migration across ridges. Disentangling these processes is crucial to understand the role of mountain ridges in shaping beta diversity across montane landscapes.

Not all mountain ridges act as barriers to species dispersal after accounting for climatic effects on habitat. In the TRR region, the Salween-Mekong divide emerges as a major dispersal barrier for plant species, even after controlling for the climatic effects at the point of habitation of species. To differentiate the geographic isolation from climatic effects, we compared observed phylogenetic beta diversity with values expected under a null model based solely on climatic factors. This approach effectively isolated the contribution of climatic isolation and confirmed the role of the Salween-Mekong divide as a geographic barrier independent of climate. Although this divide has been recognized as a significant barrier back to 1921 for fauna [46] and later for flora communities at population and genetic level [20,47], our results provide empirical support for the effectiveness of this barrier after controlling the climate impact on the habitat on each side of a range, highlighting the role of physical geography in shaping regional plant biodiversity patterns. The effectiveness of the Salween-Mekong divide acting as a dispersal barrier may be due to the large depth of the gorge in the Salween valley. The high relief of the Salween valley compressed a wide range of habitats-from tropical to alpine-into a steep elevational gradient. This compression intensifies ecological barriers, reducing the likelihood of plant dispersal across the divide. In contrast, the Mekong-Yangtze divide is less steep and with a more homogeneous and arid climate [48], resulting in fewer compressed ecological zones and a lower topographic-climate barrier for plant species. Moreover, these divides exhibit distinct patterns of geomorphic activity. The Salween-Mekong divide shows a consistent eastward direction of water-divide migration, potentially facilitating directional species transfer from the Mekong to Salween valleys. This asymmetrical movement may lead to species accumulation and promote allopatric speciation crossing the divide. The Mekong-Yangtze river does not exhibit a consistent migration direction along the divide [36,49], which could promote mixing of species pools and result in more homogeneous species assemblages across the divide. Although the role of divide migration has been mainly investigated in aquatic systems [50–53], our empirical data provide testable hypotheses regarding the influence of divide migration on plant species turnover pattern at the regional scale.

The effectiveness of mountain ridges acting as dispersal barriers is taxa dependent. Although fungal communities exhibit some spatial segregation across drainage divides, this pattern disappears once climatic factors have been accounted for. The absence of statically significant phylobeta across divides suggests that these mountain ridges may not act as geographic barriers for fungi. This could reflect the higher long-distance dispersal capacity of fungal spores compared with pollen [54], consistent with the observation that the efficiency of dispersal barrier varies with species dispersal abilities [55]. Instead, the community assembly of fungal communities depends on the environmental filtering process [56]. This result is confirmed with some global studies emphasizing climate in explaining the soil fungal diversity at regional scale [57,58]. At the regional scale, other local factors such as soil pH and calcium may filter fungal groups into different microenvironments [57]. The varied degree of isolation impact of mountain ridges is also found in other comparisons between taxa such as bird and lichen communities. The functional traits that determine dispersal abilities is likely explained by these variations [55].

Our eDNA data primarily captured species from mid-to-low elevation with implications for the efficacy of eDNA characterization of large drainage basins. The taxa detected in plant and fungal groups indicate sampling at the outlet of each drainage basin effectively recovered species at hot, dry river valleys and temperate forests at mid-elevations (Figure 2). Using documented elevation ranges for the detected genera [34], we demonstrate that the eDNA signal largely represents plant occurrence from mid-to-low elevations even under a maximum elevation preference scenario. Furthermore, our eDNA data revealed a dominance of pathogens and non-yeast unicellular fungi, which are typically associated with drylands and temperate mesic forests [58]. This observation is consistent with the known dynamics of eDNA advection, which are influenced by various biotic and abiotic factors such as DNA fragment size [59], hydrological conditions [60]. These factors contribute to varied downstream travel distances ranging from metres to hundreds of kilometres [60]. For instance, studies have demonstrated that plant eDNA is often only detected a few kilometers downstream [30,61], in contrast to the detection range for other organisms, such as invertebrates, which can extend up to 9.1 km [62]. One reason for this is that larger amplicons typically have lower abundance and decay more easily in riverine systems [59]. Therefore, our eDNA data only permits us to compare species that mainly occur in the dry river valleys and temperate forest ecosystems at lower elevations in the catchments.

Climate is the dominant factor in shaping community assembly for both plant and fungal communities, particularly for these communities within the river valley. In river valleys, general dissimilarity models reveal that climate variables explain a large proportion of phylogenetic beta diversity, especially the second factor, PC2, which captures climate constraints related to both temperature and precipitation. Similarly, the north-south segregation patterns identified through PCoA analyses show a significant division around 28^{o}N, with the pattern being especially pronounced in the Salween River for both plant and fungi communities. This segregation pattern is consistent with the 0^{o}C minimal temperature threshold in the coldest month [38], partially supporting the freezing tolerance hypothesis. This

hypothesis posits that frost tolerance acts as one of the critical physiological barriers to taxonomic shifts from tropical broadleaved forests to temperate conifer forests [38,63], demonstrating that tropical niche conservatism [64] is one of the main drivers in structuring latitudinal biodiversity gradient in the Hengduan mountains. The freezing tolerance hypothesis was initially supported using plant elevational ranges and county level distribution records [38] in the Hengduan Mountains. We documented a similar pattern with more precise community assembly data from eDNA. Certain clades, such as Urticaceae, originating from tropical Asian regions [56], have migrated northwards along river valleys until reaching their distributional limit near the 28°N freezing boundary in the Salween river valley. This pattern is less pronounced in the Mekong and Yangtze river valleys, possibly due to the drier climate in these valleys [65], which may have filtered out a high proportion of tropical lineages, resulting in more homogeneous species compositions.

Our results delineate the spatial pattern of phylogenetic and taxonomic beta diversity in the TRR region, emphasizing the varying roles of mountain ridges acting as dispersal barriers across different taxonomic groups. Our findings demonstrate the potential to extend terrestrial plant and fungal eDNA detection from soil [66] and air [67] to freshwater systems. However, the lack of species detection of upper catchment species suggests that sampling only at river outlets limits the ability to assess full basin-level biodiversity. Thus, careful sampling design is essential. In particular, increased sampling density within individual drainage basins is necessary to capture basin-level species composition more accurately [60]. Several challenges of sample plant eDNA remain, including incomplete DNA reference databases and the lack of universal primers [68]. Although our study demonstrated that ITS2 is effective for taxa identification, we can only resolve the plant and fungi communities at genus and family level respectively. To optimise riverine eDNA for plant diversity studies, it is crucial to develop comprehensive reference databases, particularly for endemic species. Moreover, better detection rates could be achieved by combining ITS2 with plastid DNA barcodes, such as ribulose-bisphosphate carboxylase (rbcL)[31]. Last but not least, the eDNA approach offers an excellent opportunity to explore multi-taxon biodiversity patterns. Including freshwater organisms such as fish, with appropriate primers like Teleo02 [69], could provide a more holistic understanding of biodiversity in the TRR region.

Conclusion

Our analyses of plant and fungi groups from riverine eDNA sampling reveal that using the ITS2 primer is sufficient to characterize the unique terrestrial plant and fungi communities in individual catchments. The habitat preference of the plant communities in eDNA samples indicates that sampling at the outlets of tributaries primarily captured mid-to-low elevation species and undersampled the upper catchments. Consistent with other genetic sampling methods[20], our results demonstrate species composition and phylogenetic beta diversity patterns are spatially structured in the Three Rivers Region, with clear segregation between the major river valleys and along the latitudinal gradient within individual river valleys. After

controlling the climate differences, only the plant community reveals a dispersal barrier associated with the Salween-Mekong divide, whereas the fungal community has not been limited by the major drainage divides in the TRR region. These findings highlight the dispersal barrier is taxa and location dependent, and this pattern will emerge only after controlling for the turnover associated with climatic differences affecting habitat. Our study offers a framework to disentangle the climate filtering process from dispersal limitation, providing a foundation for understanding how geographical configurations impact species range limits. Our eDNA approach paves the way for broader investigations of terrestrial plant and fungi groups using riverine eDNA, although further refinement of sampling methods and detection protocols would aid in optimising this technique.

Methods

Study area and sampling

The study area, defined as the Three Rivers Region (TRR), extends from 98°E to 101°E and 26.5°N to 30.2°N (Figure 1). This region includes the upper reaches of the Salween, Mekong, and Yangtze Rivers, which originate from the Tibetan Plateau. These rivers run in parallel in the TRR region, creating deep gorges up to 3000 m [35], and have nearest points within several tens of kilometres of each other. The majority of their tributaries run perpendicular to the main rivers, forming extensive alpine valley landforms. Within the defined study area, riverine environmental DNA (eDNA) samples were collected using a capsule filter from Darlly (https://darllyfiltration.com/) in May 2023 from 30 sites located at the outlets of tributaries of the Salween, Mekong, and Yangtze Rivers (Figure 1). Eight sites from the Salween and Mekong Rivers and 14 sites from the Yangtze River were sampled as the paired drainage basins on both sides of the mainstream. The sampling strategy was designed to minimise the influence of anthropogenic impact by avoiding highly impacted drainage basins. At each of the 30 sites, two replicates were collected from the outlet of each tributary. For each replicate, 20 litres of freshwater were filtered over approximately one hour. This systematic approach ensured comprehensive coverage of the riverine environments within the TRR.

eDNA Extraction, amplification, sequencing

The extraction of environmental DNA and amplification were both conducted in a dedicated laboratory. To control contamination in the extraction room, we included one extraction control by filtering tap water. We used the ITS2 primer designed by Banchi et al (2020) (forward: GAAYCATCGARTCTTTGAACGC; reverse: TCCTCCGCTTAKTGATATGC) that amplify a region of 317 base pairs on average (range 250 - 420 bp). The negative control in the amplification procedure showed no DNA template.

The eDNA extraction protocol was modified from the DNeasy Blood & Tissue Kit (Qiagen, Germany. The filter containing the buffer solution was placed on the S50 shaker for thorough

agitation. Next, the buffer solution was poured from the filter into a 50 mL centrifuge tube and centrifuged at 4500 G. Using enzyme-free pipette tips, the clear liquid was carefully removed from the surface, leaving 15 mL of liquid at the bottom of the tube. Anhydrous ethanol and 3 M sodium acetate were then added, and the mixture was stored overnight at -20 °C. The centrifuge tube was inverted to mix the contents, followed by centrifugation at 4500 G for 25 minutes, after which the supernatant was discarded. Next, 720 μL of Buffer ATL was added to each centrifuge tube, which was then agitated thoroughly for 1 minute. The resulting liquid was transferred into 2 mL centrifuge tubes. Proteinase K was added to each tube and the tubes were incubated in a 56 °C water bath. After incubation, the supernatant from the centrifuge tubes was transferred to new 2 mL centrifuge tubes, centrifuged at 13400 rpm, and the supernatant was transferred to new 2 mL centrifuge tubes. Following this, 500 μL of Buffer AL was added to each tube, mixed thoroughly, and incubated in a water bath for 10 minutes until the solution became clear. An equal volume (500 μL) of anhydrous ethanol was then added, mixed thoroughly, and briefly centrifuged. The liquid (700 μL at a time) was then pipetted and added to the spin column in multiple steps, centrifuged at 13000 rpm, and the centrifugate discarded after each step. This process was repeated until all the liquid had been centrifuged and discarded. The spin column was then washed by adding 500 μL of Buffer AW1, centrifuging for one minute at 13000 rpm, and discarding the centrifugate. This step was followed by the addition of 500 μL of Buffer AW2, centrifugation for three minutes at 17000 rpm, and discarding the centrifugate. Finally, the spin column was removed and placed in a new 1.5 mL centrifuge tube. To complete the eDNA extraction, 100 μL of Buffer AE was added to the centre of the membrane in the spin column and centrifuged for one minute at 13000 rpm.

PCR amplifications were conducted in 96-well plates following a thermocycler protocol. This protocol included an initial denaturation step at 95 °C for 30 seconds, followed by 31 cycles of denaturation at 95 °C for 30 seconds, annealing at 47 °C for 30 seconds, extension at 72 °C for 45 seconds, and a final extension step at 72 °C for 5 minutes. The 25 μL PCR system included 12.5 μL 2 × Rapid Taq Master Mix P213 (Nanjing Vazyme Biotech Co., Ltd), 1 μL 10 μM forward and reverse primers, 2 μL DNA template and 8.5 μL negative controls DEPC water. Amplification products were detected using 2% agarose gel electrophoresis, and equal volumes of these products were pooled. The pooled samples were then purified using VAHTS® DNA Clean Beads (N411, Vazyme Biotech Co., Ltd., China) protocol. Library construction was carried out with the VAHTS Universal DNA Library Prep Kit for Illumina V3 (Vazyme Biotech Co., Ltd., China) following the manufacturer's protocol, and library concentration was determined using a Qubit fluorometer (Thermo Fisher Scientific, USA). The Illumina PE150 library underwent paired-end sequencing at the Illumina sequencing facility (Shanghai Biozeron Biotechnology Co., Ltd., China).

Bioinformatic analyses

The original Illumina paired-end sequencing data were merged using the fastq_mergepairs algorithm in VSEARCH. Sequences were then split by sample barcode using the barcode_splitter script (https://bitbucket.org/princeton_genomics/barcode_splitter). For each

sample, reads were assembled with VSEARCH [70]. Sequences were demultiplexed and trimmed based on forward and reverse primer sequences using Cutadapt [71] software, with a maximum mismatch error rate of 0.1. Identical sequences were dereplicated to calculate the abundance of each sequence. The clustering of sequences into amplicon sequence variants (ASVs) was performed using the SWARM algorithm with a minimum distance of one nucleotide (d = 1). Chimeras were checked and removed using the "--uchime_denovo" command in VSEARCH [70]. Taxonomic assignment of ASVs was conducted with the ecotag tool from OBITOOLs [72], using a lowest common ancestor algorithm and a plant barcode reference database built from sequences and taxonomic information downloaded from NCBI. An in-silico PCR pipeline, utilising the algorithms obiconvert, ecopcr, obigrep, obiuniq, and obiannotate from OBITOOLs, was executed with the ITS2 primer. Parameters for the in silico PCR included a minimum length of 250 bp, a maximum length of 420 bp, and a maximum of 5 bp mismatches.

Using the checklist of native species in Yunnan [73], we generated a barcode reference database exclusively for native species. Species annotation was prioritised at 100% sequence similarity and was performed solely at the species level. For ASVs that could not be annotated to the species level, a secondary annotation was conducted using the original barcode reference database. In this secondary process, sequences with 97% or higher similarity to the reference were identified at the species level, sequences with 95-97% similarity at the genus level, sequences with 90-95% similarity at the family level, and sequences with less than 90% similarity at the order level. For all ASVs with specific names, we used TaxonKit [74], a cross-platform and efficient NCBI taxonomy toolkit [74], to load lineage information for each unique sequence. ASVs with lengths shorter than 250 bp or longer than 420 bp, not assigned to a plant and fungi group, or with an abundance frequency below 0.001 were removed to avoid tag-jump noise [67]. The LULU algorithm [75] was then applied to clean ASVs, identifying errors based on sequence identity, abundance, and co-occurrence patterns. Each ASV was classified as a contaminant or not based on contamination signatures from previous studies. Only curated ASVs detected in more than 10 reads were retained. ASV reads from two replicates were assembled on the species checklist at each site. Finally, we chose the classes "Magnoliopsida" and "Pinopsida" as the plant group and divisions "Basidiomycota", "Ascomycota", "Chytridiomycota", "Mucoromycota", "Olpidiomycota", "Blastocladiomycota", "Zoopagomycota" as fungi group. We chose to focus on the entire fungi kingdom, rather than just macro-fungi, because only 53 macro-fungi species were detected across 18 sites, which was insufficient for identifying biodiversity patterns.

Plant genera-level elevational information and fungi function types

To understand the habitat preference for the plant and fungi species detected in the eDNA samples, we extract elevational preference for plants from flora and function types for fungal from published data. For plants taxa detected in the eDNA samples, we extract genus level elevational information from the flora of China (http://www.efloras.org/flora_page.aspx?flora_id=2) and local floras including Tibet, Sichuan, and Yunnan floras (Wu, 1986; Wu, 1987; Zhou, 1994; Wang, 1994). The elevation

information includes maximum and minimal elevation preference at genus level. Then genus and family level elevation information was aggregated from these species level information. The elevation information covers 85%, 87%, and 84% of sampled plant sequences in the Mekong, Salween, and Yangtze respectively. We perform a density plot between the elevation in each drainage basin and the mean, minimal, and maximum elevation for sampled plant species in each drainage basin and compute the overlap density using the overlap function in the overlapping package [76]. Besides, the functional type of fungal species was extracted from [58], including the arbuscular mycorrhizal (AM), ectomycorrhizal fungi (EcM), molds (Mold), nonmycorrhizal Agaricomycetes (AgarNM; mainly saprotrophic macrofungi), nonsymbiotically biotrophic group on a wide variety of organisms (Path), yeasts (Yeast), nonyeast unicellular fungi (Unicell), and opportunistic human pathogens (OHP). We extracted family-level taxonomic information and matched it with the corresponding functional types.

Plant and fungi taxonomic and phylogenetic diversity

The genus level vascular plant phylogeny was derived from Dimitrov et al., 2023 [77], including 135 genera in angiosperm and four genera (i.e., Pinus, Abies, Cupressus, and Torreya) in gymnosperm. For the fungi phylogeny, we derived family level fungi phylogeny from Li et al [78] which includes 68 families. We choose genus level for plant and family level for fungi as it could better represent evolutionary history and has good enough resolution to capture more taxa. In the OTU table, the taxonomic level under genus and family level in plant and fungi was merged into the genus and family level, respectively. For the OTU table can only be assigned into the higher level, we choose one genus or family within a certain clade to represent the family or genus. This approach is based on the hypothesis that each genus or family forms a clade (a monophyletic group) where species have diverged from their common ancestor over the same period in the phylogeny. Therefore, the choice of one species over another does not modify the phylogenetic turnover pattern (Rozanski *et al*. 2022). We calculated the pairwise Sorensen dissimilarity for both taxonomic diversity and phylogenetic beta diversity. These beta diversity metrics only consider the presence/absence of each ASV in certain basin and were computed in the phylo_beta and beta_diss function for phylogenetic and taxonomic diversity respectively in the phyloregion package in R [79].

Beta diversity and PCoA analyses

We performed the two-dimensional Principal Coordination Analysis (PCoA) based on a Sorensen beta matrix using the pcoa function in the ape package [80]. We then extracted the first two axes of the PCoA to calculate dissimilarity and computed ellipses for the ordination plot with stat_ellipse function from ggplot2 v.3.5.0 [81] considering a multivariate t-distribution at the 0.95 level. The PCoA results are also visualized spatially for the first two axes of PCoA analysis. The PCoA analyses are computed and visualized for both phylogenetic and taxonomic Sorensen beta diversities.

Climate variables

We obtained 31 bioclimatic variables from 1981 to 2010 from the CHELSA climate model [82]. Climate layers in this model include a wide range of biologically important variables for plants. We extract climate values for sampled drainage basins and computed principal components from the correlation matrix of these climate layers (Fig. S7). The first two axes of the PCA capture more than 80% of variation in the sampling drainage basins. We extract the scores from the first two axes in the PCA for each sampling basin and use them for the generalized dissimilarity model. This method should include sufficient climate variables to accurately reflect energy and water availability constraints and also ensures the dimension of orthogonal climate axes. We also computed the climate variable for the sub-basins where the area is over the sampling points of 1000m to conduct the sensitivity analyses and this approach does not change the model results.

Generalized dissimilarity model within and across divide

A generalized dissimilarity model (GDM; [83,84] was used on the Sorensen dissimilarity matrix for both phylogenetic and taxonomic beta diversity to build the climate driven GDM model. In the GDM, we split drainage basin pairs into background pairs and testing pairs. We first select pairs not crossing main drainage divides and within river valleys (i.e. Salween, Mekong, and Yangtze River valleys) to construct the null model. The assumption of the null model is that only climate and geographic distance impact the beta diversity within river valleys. The climate distance was calculated from PC1 and PC2 from the PCA analyses. The geographic distance was computed from the sampling coordinates directly. The GDM was implemented using the gdm package in R with a spline and knot of 3 [84]. After calibrating the dissimilarity model for all pairs within river valleys, we used the model to predict turnover for pairs that lie on either side of the Salween-Mekong divide, the Mekong-Yangtze divide, or the Salween-Mekong-Yangtze divide. This prediction represents the beta diversity purely due to climate change between sites. Finally, we compared the observed beta and the beta diversity from this model. Any observed beta diversity that is significantly higher than the predicted beta diversity is regarded as being due to the barrier effect of the major drainage divides. We used the Wilcoxon t-test to test if there is a significant difference between the observed and predicted beta diversity as this test uses the rank based test and without the assumption of a normal distribution [85].

Topographic analyses

Averaged topographic swath profiles corresponding to the elevation of a west-to-east transect across the TRR region. Each swath was taken connecting the sampling basins in each river valley, crossing Salween, Mekong, and Yangtze rivers. In total, four swath profiles were made to report topographic change in the north, middle and south of the TRR region.

Acknowledgements

We thank the State Key Laboratory of Water Pollution Control and Green Resource Recycling in Nanjing University for providing lab space and consumables for the lab work. We thank Xianjun Fang for providing the catchment shapefile in the TRR region, Song Zhang, Siyuan Gu for providing help in the fieldwork. YC, WS, LP, and NEZ acknowledge financial support from ETH Zürich (ETH+ grant Biodiversity, Earth, Climate Coupling in Yunnan). Open access funding provided by Eidgenossische Technische Hochschule Zurich.

Reference

1. Rahbek, C. *et al.* Humboldt's enigma: What causes global patterns of mountain biodiversity? *Science* **365**, 1108–1113 (2019).
2. Fjeldså, J., Bowie, R. C. K. & Rahbek, C. The Role of Mountain Ranges in the Diversification of Birds. *Annu. Rev. Ecol. Evol. Syst.* **43**, 249–265 (2012).
3. Sonne, J. & Rahbek, C. Idiosyncratic patterns of local species richness and turnover define global biodiversity hotspots. *Proc. Natl. Acad. Sci.* **121**, e2313106121 (2024).
4. Janzen, D. H. Why Mountain Passes are Higher in the Tropics. *Am. Nat.* **101**, 233–249 (1967).
5. Rahbek, C. The Relationship Among Area, Elevation, And Regional Species Richness In Neotropical Birds. *Am. Nat.* (1997) doi:10.1086/286028.
6. Hazzi, N. A., Moreno, J. S., Ortiz-Movliav, C. & Palacio, R. D. Biogeographic regions and events of isolation and diversification of the endemic biota of the tropical Andes. *Proc. Natl. Acad. Sci.* **115**, 7985–7990 (2018).
7. Keddy, P. A. Assembly and response rules: two goals for predictive community ecology. *J. Veg. Sci.* **3**, 157–164 (1992).
8. He, J. *et al.* Joint effects of environmental filtering and dispersal limitation on the species assemblage of the Tibetan Plateau. *J. Biogeogr.* **49**, 640–653 (2022).
9. Purcell, J. & Avilés, L. Gradients of precipitation and ant abundance may contribute to the altitudinal range limit of subsocial spiders: insights from a transplant experiment. *Proc. R. Soc. B Biol. Sci.* **275**, 2617–2625 (2008).
10. Normand, S. *et al.* Importance of abiotic stress as a range-limit determinant for European plants: insights from species responses to climatic gradients. *Glob. Ecol. Biogeogr.* **18**, 437–449 (2009).
11. Baselga, A., Lobo, J. M., Svenning, J.-C. & Araújo, M. B. Global patterns in the shape of species geographical ranges reveal range determinants. *J. Biogeogr.* **39**, 760–771 (2012).

12. White, A. E. Geographical Barriers and Dispersal Propensity Interact to Limit Range Expansions of Himalayan Birds. *Am. Nat.* **188**, 99–112 (2016).
13. Liu, Y., Wang, Y., Willett, S. D., Zimmermann, N. E. & Pellissier, L. Escarpment evolution drives the diversification of the Madagascar flora. *Science* (2024) doi:10.1126/science.adi0833.
14. Stein, A., Gerstner, K. & Kreft, H. Environmental heterogeneity as a universal driver of species richness across taxa, biomes and spatial scales. *Ecol. Lett.* **17**, 866–880 (2014).
15. Sánchez-Montes, G., Wang, J., Ariño, A. H. & Martínez-Solano, Í. Mountains as barriers to gene flow in amphibians: Quantifying the differential effect of a major mountain ridge on the genetic structure of four sympatric species with different life history traits. *J. Biogeogr.* **45**, 318–331 (2018).
16. Leugger, F. *et al.* Dispersal and habitat dynamics shape the genetic structure of the Northern chamois in the Alps. *J. Biogeogr.* **49**, 1848–1861 (2022).
17. Machado, A. P., Clément, L., Uva, V., Goudet, J. & Roulin, A. The Rocky Mountains as a dispersal barrier between barn owl (Tyto alba) populations in North America. *J. Biogeogr.* **45**, 1288–1300 (2018).
18. Cuypers, L. N. *et al.* Biogeographical Importance of the Livingstone Mountains in Southern Tanzania: Comparative Genetic Structure of Small Non-volant Mammals. *Front. Ecol. Evol.* **9**, (2022).
19. Wei, X., Meng, H. & Jiang, M. Landscape Genetic Structure of a Streamside Tree Species Euptelea pleiospermum (Eupteleaceae): Contrasting Roles of River Valley and Mountain Ridge. *PLOS ONE* **8**, e66928 (2013).
20. Liu, J. *et al.* Geological and ecological factors drive cryptic speciation of yews in a biodiversity hotspot. *New Phytol.* **199**, 1093–1108 (2013).
21. He, K. *et al.* Cryptic phylogeographic history sheds light on the generation of species diversity in sky-island mountains. *J. Biogeogr.* **46**, 2232–2247 (2019).
22. Sonkoly, J. *et al.* Do large-seeded herbs have a small range size? The seed mass–distribution range trade-off hypothesis. *Ecol. Evol.* **7**, 11204–11212 (2017).

718 23. Aslan, C. *et al.* Employing plant functional groups to advance seed dispersal ecology
719 and conservation. *AoB PLANTS* **11**, plz006 (2019).
720 24. Normand, S. *et al.* Postglacial migration supplements climate in determining plant
721 species ranges in Europe. *Proc. R. Soc. B Biol. Sci.* **278**, 3644–3653 (2011).
722 25. Seymour, M. *et al.* Executing multi-taxa eDNA ecological assessment via traditional
723 metrics and interactive networks. *Sci. Total Environ.* **729**, 138801 (2020).
724 26. Marques, V. *et al.* Blind assessment of vertebrate taxonomic diversity across spatial
725 scales by clustering environmental DNA metabarcoding sequences. *Ecography* **43**,
726 1779–1790 (2020).
727 27. Zong, S. *et al.* Combining environmental DNA with remote sensing variables to map fish
728 species distributions along a large river. (2023).
729 28. Sales, N. G. *et al.* Fishing for mammals: Landscape-level monitoring of terrestrial and
730 semi-aquatic communities using eDNA from riverine systems. *J. Appl. Ecol.* **57**, 707–716
731 (2020).
732 29. Reji Chacko, M. *et al.* Catchment-based sampling of river eDNA integrates terrestrial and
733 aquatic biodiversity of alpine landscapes. *Oecologia* **202**, 699–713 (2023).
734 30. Espinosa Prieto, A., Beisel, J.-N., Verschuren, P. & Hardion, L. Toward freshwater plant
735 diversity surveys with eDNA barcoding and metabarcoding. *Environ. DNA* **5**, 648–670
736 (2023).
737 31. Espinosa Prieto, A., Hardion, L., Debortoli, N. & Beisel, J.-N. Finding the perfect pairs: A
738 matchmaking of plant markers and primers for multi-marker eDNA metabarcoding. *Mol.*
739 *Ecol. Resour.* **24**, e13937 (2024).
740 32. Ariza, M. *et al.* Plant biodiversity assessment through soil eDNA reflects temporal and
741 local diversity. *Methods Ecol. Evol.* **14**, 415–430 (2023).
742 33. Johnson, M. D., Cox, R. D. & Barnes, M. A. The detection of a non-anemophilous plant
743 species using airborne eDNA. *PLOS ONE* **14**, e0225262 (2019).
744 34. Chang, Y. *et al.* Phytodiversity is associated with habitat heterogeneity from Eurasia to
745 the Hengduan Mountains. *New Phytol.* **240**, 1647–1658 (2023).

35. Yang, R. *et al.* Spatial and temporal pattern of erosion in the Three Rivers Region, southeastern Tibet. *Earth Planet. Sci. Lett.* **433**, 10–20 (2016).
36. Gelwick, K. D., Willett, S. D. & Yang, R. Geomorphic indicators of continental-scale landscape transience in the Hengduan Mountains, SE Tibet, China. *Earth Surf. Dyn.* **12**, 783–800 (2024).
37. Zhang, D.-R. *et al.* Shared response to changes in drainage basin: Phylogeography of the Yunnan small narrow-mouthed frog, Glyphoglossus yunnanensis (Anura: Microhylidae). *Ecol. Evol.* **10**, 1567–1580 (2020).
38. Li, Q. *et al.* Grade of Membership models reveal geographical and environmental correlates of floristic structure in a temperate biodiversity hotspot. *New Phytol.* **232**, 1424–1435 (2021).
39. Martín-Devasa, R., Jiménez-Valverde, A., Leprieur, F., Baselga, A. & Gómez-Rodríguez, C. Dispersal limitation shapes distance-decay patterns of European spiders at the continental scale. *Glob. Ecol. Biogeogr.* **33**, e13810 (2024).
40. Rana, S. K., Luo, D., Rana, H. K., O'Neill, A. R. & Sun, H. Geoclimatic factors influence the population genetic connectivity of Incarvillea arguta (Bignoniaceae) in the Himalaya–Hengduan Mountains biodiversity hotspot. *J. Syst. Evol.* **59**, 151–168 (2021).
41. Novillo, A. *et al.* Beta diversity patterns in Andean rodents: current and historical factors as drivers of turnover and nestedness. *J. Mammal.* **105**, 230–240 (2024).
42. Padullés Cubino, J., Chytrý, M., Divíšek, J. & Jiménez-Alfaro, B. Climatic filtering and temporal instability shape the phylogenetic diversity of European alpine floras. *Ecography* **2022**, e06316 (2022).
43. Chen, X., Zhou, T., Wu, P. & Roberts, M. J. Better Resolved Orography Improves Precipitation Simulation Over the Tibetan Plateau in High-Resolution Models. *J. Geophys. Res. Atmospheres* **129**, e2024JD041140 (2024).
44. Stanik, N., Peppler-Lisbach, C. & Rosenthal, G. Extreme droughts in oligotrophic mountain grasslands cause substantial species abundance changes and amplify community filtering. *Appl. Veg. Sci.* **24**, e12617 (2021).

45. Xiang, R. *et al.* Assessing the Regional Climate Response to Different Hengduan Mountains Geometries With a High-Resolution Regional Climate Model. *J. Geophys. Res. Atmospheres* **129**, e2023JD040208 (2024).
46. Ward, F. K. The Mekong-Salween Divide as a Geographical Barrier. *Geogr. J.* **58**, 49–56 (1921).
47. Luo, D., Xu, B., Li, Z.-M. & Sun, H. The 'Ward Line–Mekong–Salween Divide' is an important floristic boundary between the eastern Himalaya and Hengduan Mountains: evidence from the phylogeographical structure of subnival herbs Marmoritis complanatum (Lamiaceae). *Bot. J. Linn. Soc.* **185**, 482–496 (2017).
48. Gao, F., Tan, X., Zhou, C., Bian, S. & Shi, F. Eastward drainage-divide migrations driven by the spatial variations in precipitation and tectonic uplift contribute to the formation of the Parallel Rivers in the Hengduan Mountains, Southeastern Tibet. *Geomorphology* **468**, 109513 (2025).
49. Cao, K. *et al.* Southwestward growth of plateau surfaces in eastern Tibet. *Earth-Sci. Rev.* **232**, 104160 (2022).
50. Waters, J. M., Craw, D., Youngson, J. H. & Wallis, G. P. GENES MEET GEOLOGY: FISH PHYLOGEOGRAPHIC PATTERN REFLECTS ANCIENT, RATHER THAN MODERN, DRAINAGE CONNECTIONS. *Evolution* **55**, 1844–1851 (2001).
51. Waters, J. M., Wallis, G. P., Burridge, C. P. & Craw, D. Geology shapes biogeography: Quaternary river-capture explains New Zealand's biologically 'composite' Taieri River. *Quat. Sci. Rev.* **120**, 47–56 (2015).
52. Bossu, C. M., Beaulieu, J. M., Ceas, P. A. & Near, T. J. Explicit tests of palaeodrainage connections of southeastern North America and the historical biogeography of Orangethroat Darters (Percidae: Etheostoma: Ceasia). *Mol. Ecol.* **22**, 5397–5417 (2013).
53. He, C. *et al.* Drainage divide migration and implications for climate and biodiversity. *Nat. Rev. Earth Environ.* **5**, 177–192 (2024).
54. Fichant, T., Ledent, A., Collart, F. & Vanderpoorten, A. Dispersal capacities of pollen, seeds and spores: insights from comparative analyses of spatial genetic structures in

802 bryophytes and spermatophytes. *Front. Plant Sci.* **14**, (2023).
803 55. Peña, R., Obeso, J. R. & Laiolo, P. Dispersal constrains the biotic connectivity of
804 mountain assemblages. *J. Biogeogr.* **51**, 1230–1243 (2024).
805 56. Huang, X. *et al.* Tropical Asian Origin, boreotropical migration and long-distance
806 dispersal in Nettles (Urticeae, Urticaceae). *Mol. Phylogenet. Evol.* **137**, 190–199 (2019).
807 57. Tedersoo, L. *et al.* Global diversity and geography of soil fungi. *Science* **346**, 1256688
808 (2014).
809 58. Mikryukov, V. *et al.* Connecting the multiple dimensions of global soil fungal diversity.
810 *Sci. Adv.* **9**, eadj8016 (2023).
811 59. Jo, T. *et al.* Rapid degradation of longer DNA fragments enables the improved
812 estimation of distribution and biomass using environmental DNA. *Mol. Ecol. Resour.* **17**,
813 e25–e33 (2017).
814 60. Carraro, L., Stauffer, J. B. & Altermatt, F. How to design optimal eDNA sampling
815 strategies for biomonitoring in river networks. *Environ. DNA* **3**, 157–172 (2021).
816 61. d'Auriac, M. B. A., Strand, D. A., Mjelde, M., Demars, B. O. L. & Thaulow, J. Detection of
817 an invasive aquatic plant in natural water bodies using environmental DNA. *PLOS ONE*
818 **14**, e0219700 (2019).
819 62. Deiner, K. & Altermatt, F. Transport Distance of Invertebrate Environmental DNA in a
820 Natural River. *PLOS ONE* **9**, e88786 (2014).
821 63. Zanne, A. E. *et al.* Three keys to the radiation of angiosperms into freezing
822 environments. *Nature* **506**, 89–92 (2014).
823 64. Wiens, J. J. & Donoghue, M. J. Historical biogeography, ecology and species richness.
824 *Trends Ecol. Evol.* **19**, 639–644 (2004).
825 65. Fan, H. & He, D. Temperature and Precipitation Variability and Its Effects on Streamflow
826 in the Upstream Regions of the Lancang–Mekong and Nu–Salween Rivers. *J.*
827 *Hydrometeorol.* **16**, 2248–2263 (2015).
828 66. Barnes, C. J. *et al.* Metabarcoding of soil environmental DNA replicates plant community
829 variation but not specificity. *Environ. DNA* **4**, 732–746 (2022).

67. Banchi, E. *et al.* Environmental DNA assessment of airborne plant and fungal seasonal diversity. *Sci. Total Environ.* **738**, 140249 (2020).
68. Kress, W. J. Plant DNA barcodes: Applications today and in the future. *J. Syst. Evol.* **55**, 291–307 (2017).
69. Duarte, I. A. *et al.* Short-term variability of fish condition and growth in estuarine and shallow coastal areas. *Mar. Environ. Res.* **134**, 130–137 (2018).
70. Rognes, T., Flouri, T., Nichols, B., Quince, C. & Mahé, F. VSEARCH: a versatile open source tool for metagenomics. *PeerJ* **4**, e2584 (2016).
71. Martin, M. Cutadapt removes adapter sequences from high-throughput sequencing reads. *EMBnet.journal* **17**, 10–12 (2011).
72. Boyer, F. *et al.* obitools: a unix-inspired software package for DNA metabarcoding. *Mol. Ecol. Resour.* **16**, 176–182 (2016).
73. Sun, H. & Gao, Z. *YUNNANSHENG SHENGWU WUZHONG MINGLU*. (Yunnan technology publisher, 2016).
74. Shen, W. & Ren, H. TaxonKit: A practical and efficient NCBI taxonomy toolkit. *J. Genet. Genomics* **48**, 844–850 (2021).
75. Frøslev, T. G. *et al.* Algorithm for post-clustering curation of DNA amplicon data yields reliable biodiversity estimates. *Nat. Commun.* **8**, 1188 (2017).
76. Pastore, M. Overlapping: a R package for Estimating Overlapping in Empirical Distributions. *J. Open Source Softw.* **3**, 1023 (2018).
77. Dimitrov, D. *et al.* Diversification of flowering plants in space and time. *Nat. Commun.* **14**, 7609 (2023).
78. Li, Y. *et al.* A genome-scale phylogeny of the kingdom Fungi. *Curr. Biol.* **31**, 1653-1665.e5 (2021).
79. Daru, B. H., Karunarathne, P. & Schliep, K. phyloregion: R package for biogeographical regionalization and macroecology. *Methods Ecol. Evol.* **11**, 1483–1491 (2020).
80. Paradis, E. *et al.* ape: Analyses of Phylogenetics and Evolution. 5.8 https://doi.org/10.32614/CRAN.package.ape (2002).

81. Wickham, H. ggplot2. *WIREs Comput. Stat.* **3**, 180–185 (2011).
82. Karger, D. N. *et al.* Climatologies at high resolution for the earth's land surface areas. *Sci. Data* **4**, 170122 (2017).
83. Ferrier, S., Manion, G., Elith, J. & Richardson, K. Using generalized dissimilarity modelling to analyse and predict patterns of beta diversity in regional biodiversity assessment. *Divers. Distrib.* **13**, 252–264 (2007).
84. Mokany, K., Ware, C., Woolley, S. N. C., Ferrier, S. & Fitzpatrick, M. C. A working guide to harnessing generalized dissimilarity modelling for biodiversity analysis and conservation assessment. *Glob. Ecol. Biogeogr.* **31**, 802–821 (2022).
85. Fay, M. P. & Proschan, M. A. Wilcoxon-Mann-Whitney or t-test? On assumptions for hypothesis tests and multiple interpretations of decision rules. *Stat. Surv.* **4**, 1–39 (2010).

Appendix

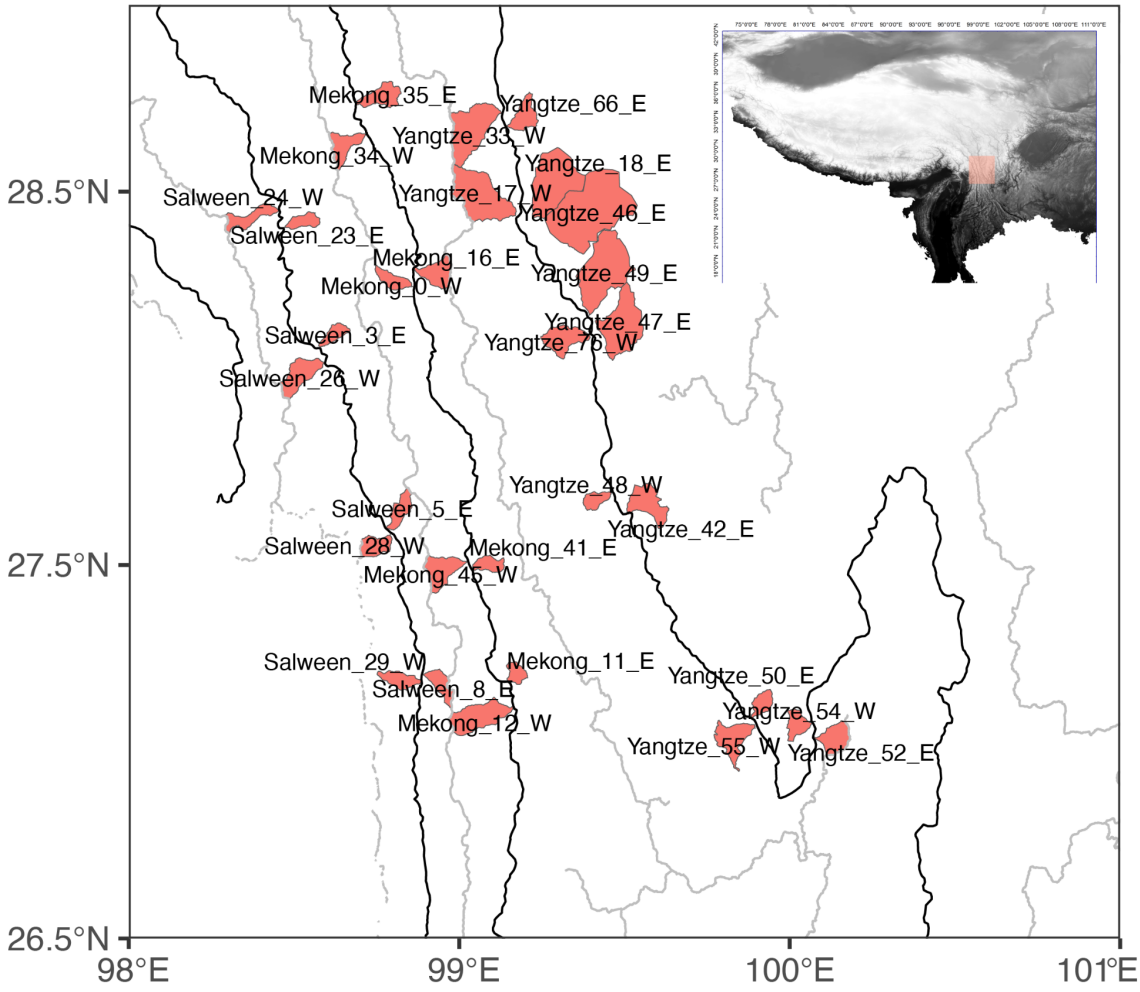

Figure S1. sampling location and sampling name

Figure S2. heatmap for the plant genera that are detected from sampling locations

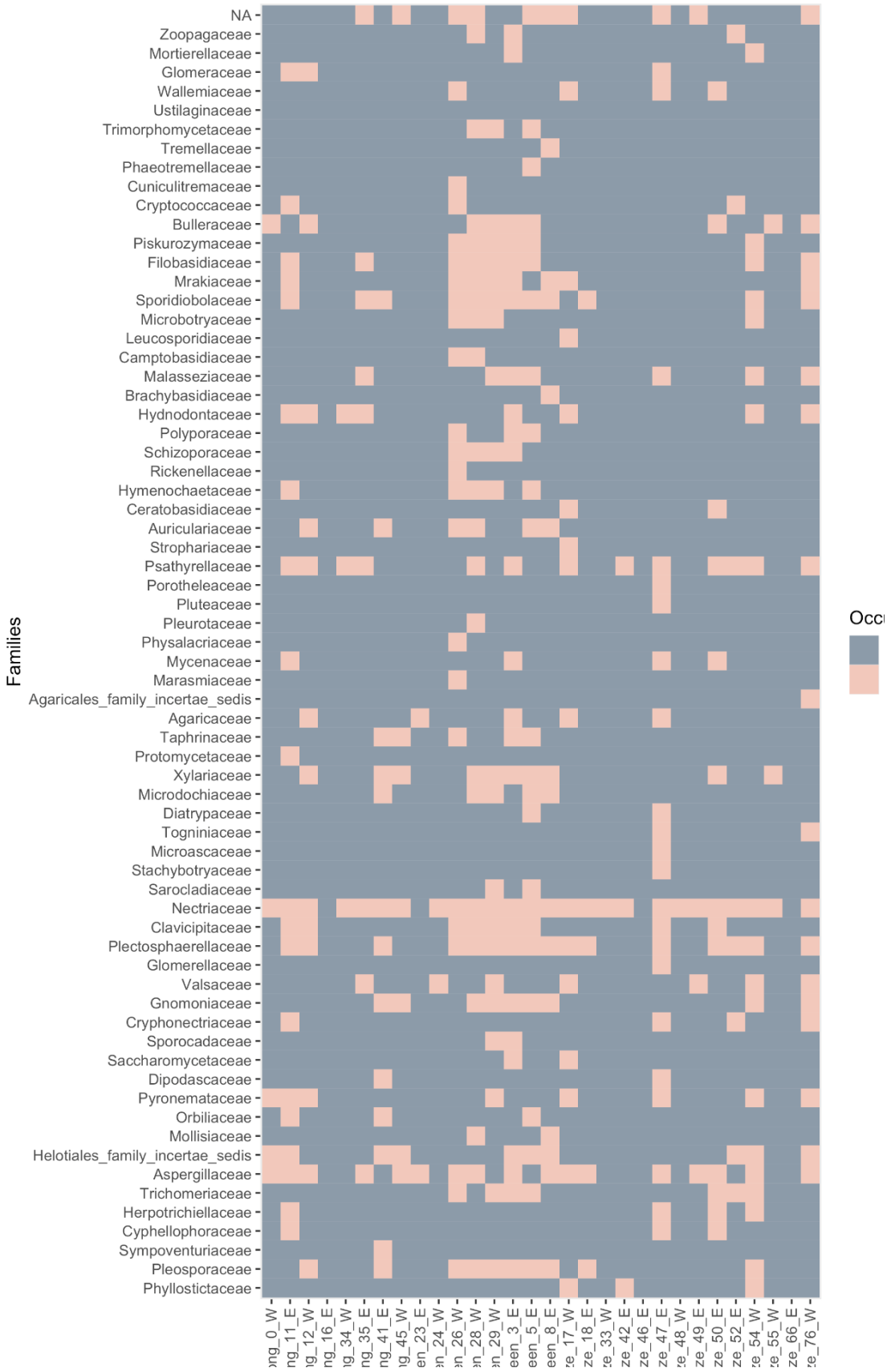

Figure S3. heatmap for the fungi families that are detected from sampling locations

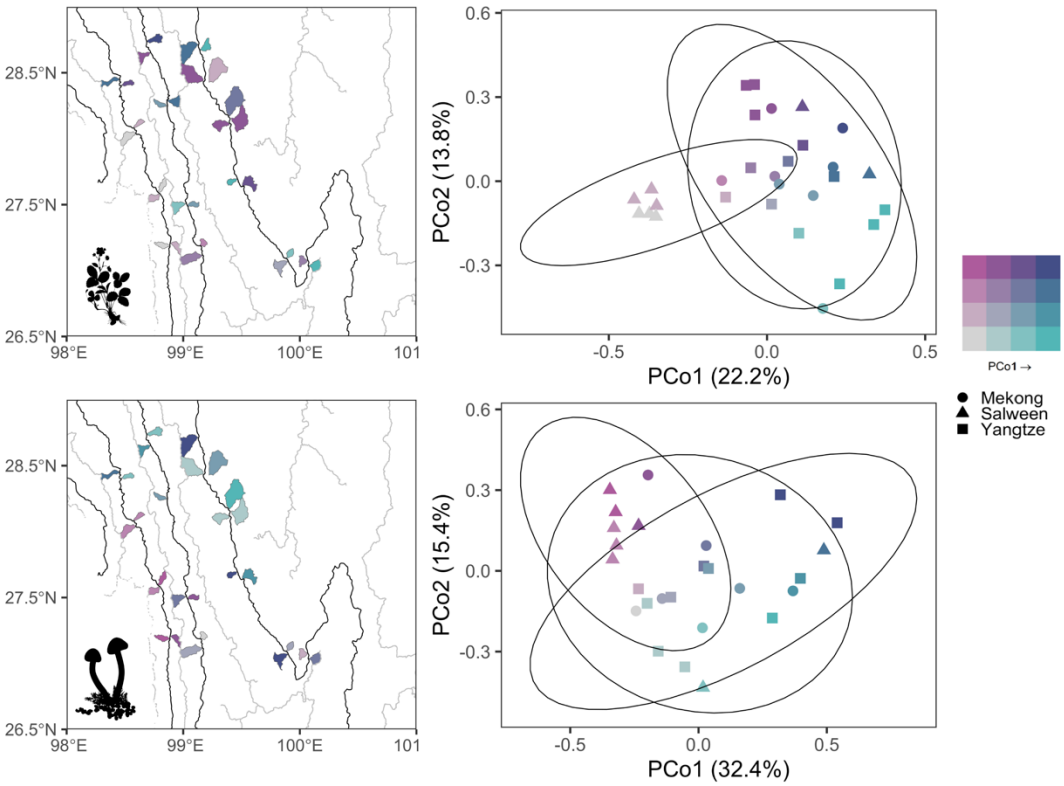

Figure S4 Species composition of vascular plants and fungi on biplot maps and pcoa ordinary plots based on Sorensen taxonomic beta diversity. Figures (a) and (c) represent the spatial distribution of the first two PCoA axes in plants and fungi, respectively; colour gradients highlight the species composition difference between different drainage basins. Black lines represent the river valleys and grey lines represent mountain ridges. S represents the Salween River, M represents the Mekong River, and Y represents the Yangtze River. The second column represents the PCoA ordination of species composition in the Salween, Mekong and Yangtze Rivers. The colour of the points corresponds to the color in the drainage basins in the left panel. Circles represent the Mekong River, triangles the Salween River, and squares the Yangtze River. Data ellipses were computed for the ordination plot considering a multivariate t-distribution with a 0.95 level. The silhouette images were derived from phylopic (https://www.phylopic.org).

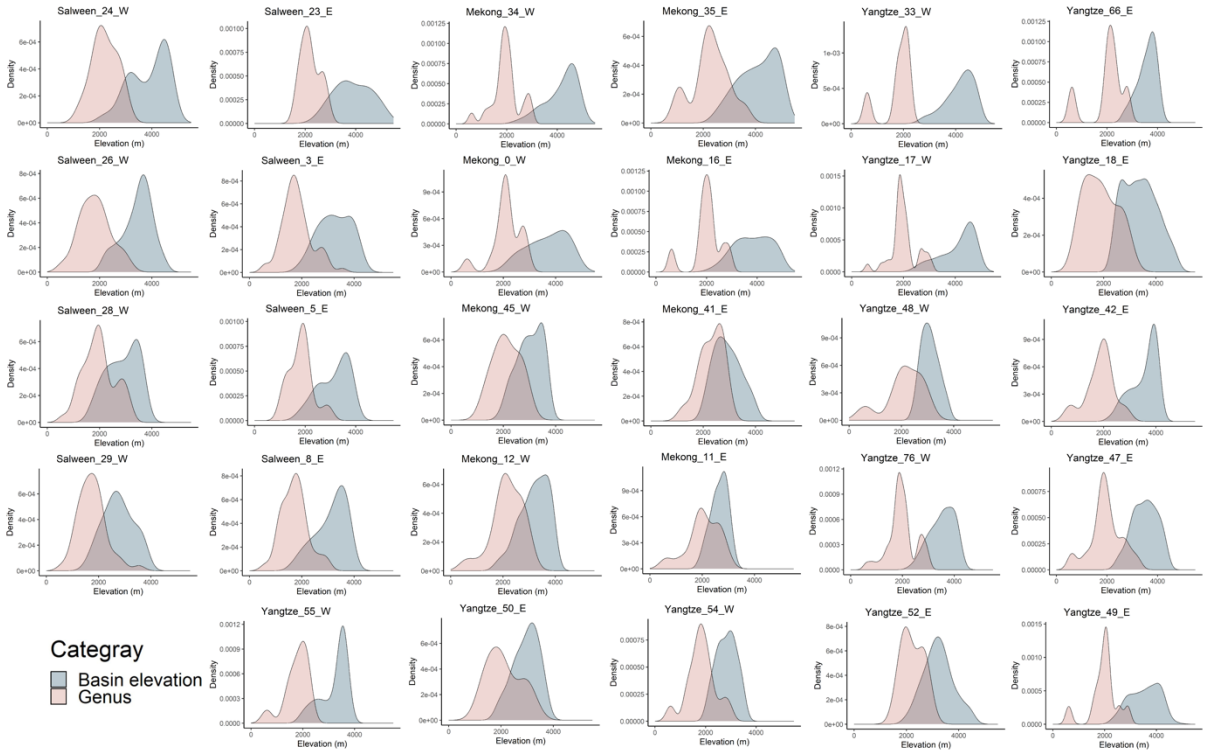

Figure S5. Elevation density plots with the sampled genus and family level mean elevation preference (pink) and drainage basins elevation range (grey), in all sampling sites across Salween, Mekong and Yangtze Rivers.

`

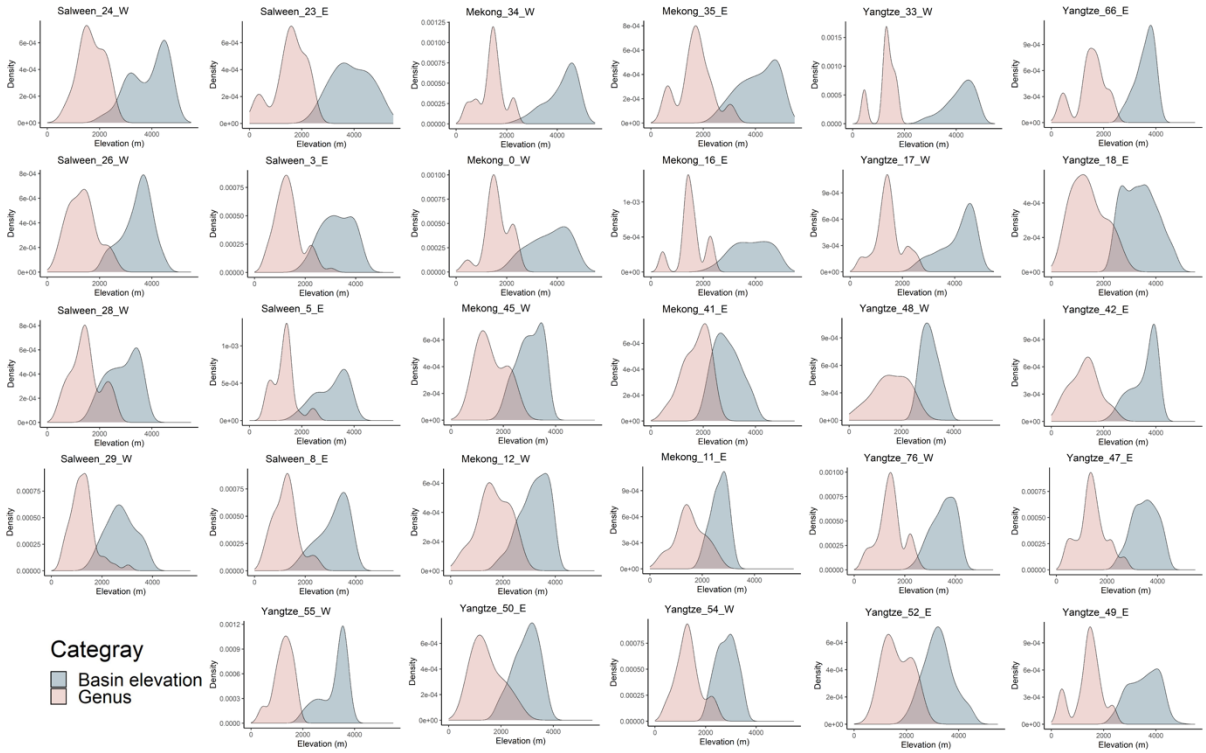

Figure S6. Elevation density plots with the sampled genus and family level minimal elevation preference (pink) and drainage basins elevation range (grey), in all sampling sites across Salween, Mekong and Yangtze Rivers.

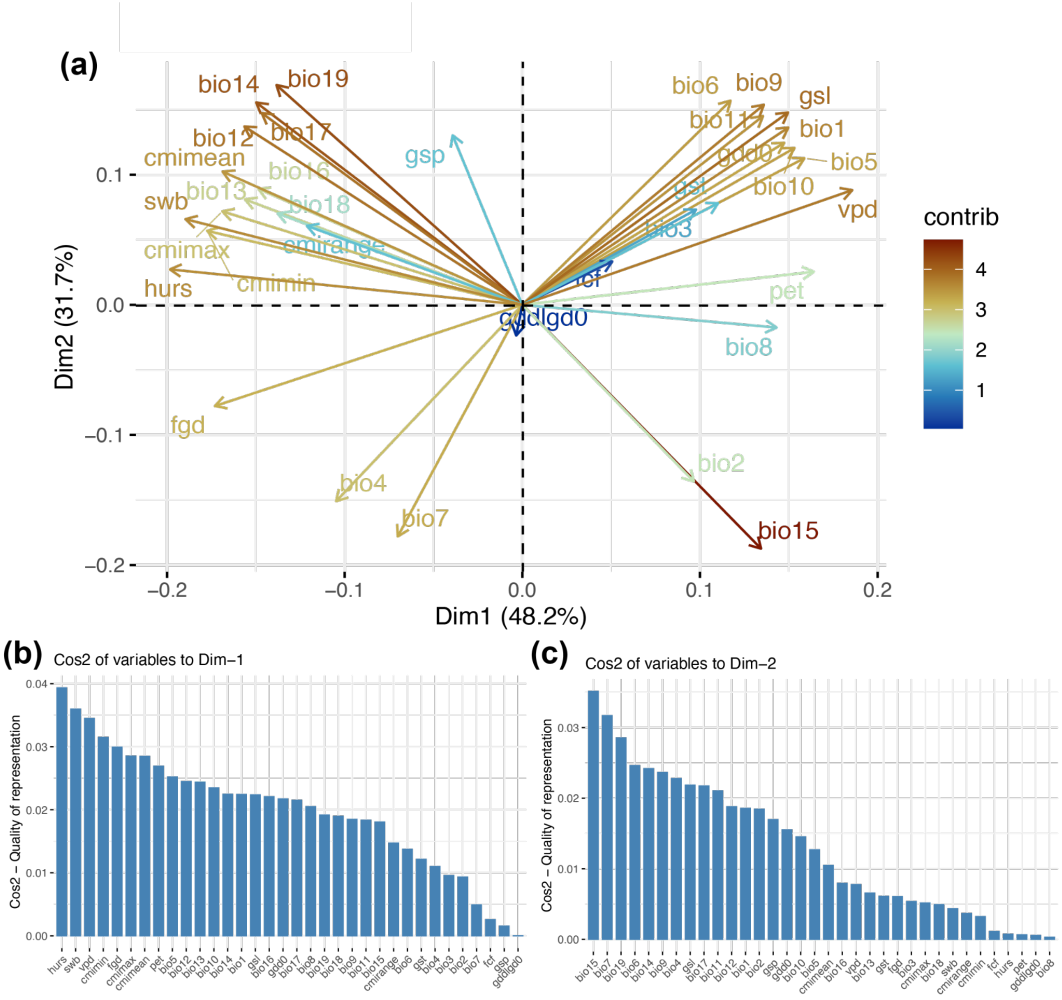

Figure S7. The climate conditions in terms of growing degree days (gdd; a) and precipitation at driest month (bio14, b) in the TRR region. The units of gdd is °C day, and the units of bio14 is kg m^{-2} $month^{-1}$.

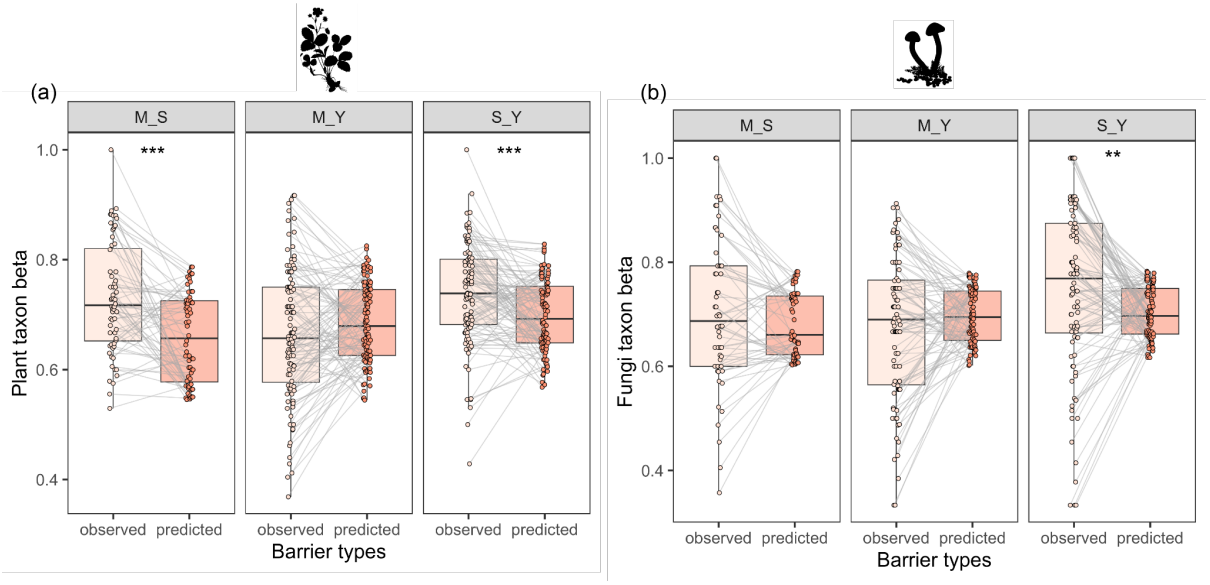

Figure S8. The comparison between climate and geographic distance predicted taxonomic beta diversity versus observed phylogenetic beta diversity across different mountain ridges in both plant (a) and fungi (b) communities. Note that M_S represents the Salween-Mekong drainage divide; M_Y represents the Mekong-Yangtze divide; and S_Y represents the Salween-Mekong-Yangtze divide. Star signs represent the significance level from Wilcox comparison (i.e. p<0.001***; p<0.01**; p<0.05*)

Table S1. the summary of detected species

Kingdom	Phylum	Class	Order	Family	Genus	Species	subspecies	no rank
Plant	8			33	139	105	7	
Fungi	3	10	7	87	76	111		5

Table S2. The top five plant families in different river valleys

Salween		Mekong		Yangtze	
Family	prop	Family	prop	Family	prop
Urticaceae	9.0	Fabaceae	7.5	Fabaceae	14.9
Betulaceae	6.0	Asteraceae	7.5	Poaceae	11.9
Araliaceae	6.0	Urticaceae	6.0	Asteraceae	9.0
Saxifragaceae	4.5	Poaceae	6.0	Urticaceae	6.0
Rosaceae	4.5	Betulaceae	6.0	Rosaceae	6.0

Table S3. The top five functional groups of fungal communities in different river valleys. Func_group represents the functional group, Prop represents the proportion of these functional groups. The abbreviation shows arbuscular mycorrhizal (AM), ectomycorrhizal fungi (EcM), molds (Mold), nonmycorrhizal Agaricomycetes (AgarNM; mainly saprotrophic

967 macrofungi), nonsymbiotically biotrophic group on a wide variety of organisms (Path), yeasts
968 (Yeast), nonyeast unicellular fungi (Unicell), and opportunistic human pathogens (OHP).
969
970

Salween		Mekong		Yangtze	
Func_group	Prop	Func_group	Prop	Func_group	Prop
Path	28.6	Path	30	Path	28.8
Unicell	17.2	Unicell	25.6	Unclassified	18.7
Unclassified	16.8	Unclassified	21.1	Unicell	18.3
Yeast	13	OHP	8.9	OHP	13
AgarNM	12.6	AgarNM	7.8	AgarNM	8.2

971
972
973 **Table S4**, the summary of generalized dissimilarity model for both plant and fungi
974 communities

	explained deviance(%)	first predictor	coefficient	second predictor	coefficient	third predictor	coefficient
plant phylobeta	13.55	PC2	0.44	PC1	0.11	distance	0
fungi phylobeta	6.21	PC2	0.40	PC1	0.03	distance	0
plant taxon beta	17.98	PC2	0.78	PC1	0.24	distance	0
fungi taxon beta	7.11	PC2	0.61	PC1	0.08	distance	0

975
976